Journal of Geodesy (2001) 74: 773–782

Journal of Geodesy
© Springer-Verlag 2001

Implementation of multigrid solvers for satellite gravity anomaly recovery

J. Kusche

Institute for Theoretical Geodesy, University of Bonn, Nußallee 17, D-53115 Bonn, Germany
e-mail: kusche@uni-bonn.de; Tel.: +49-228-733578; Fax: +49-228-733029

Received: 4 February 2000 / Accepted: 15 September 2000

Abstract. Dedicated SST – or gradiometry missions like GRACE and GOCE will provide gravity field information of unprecedented resolution and precision. It has been recognized that better gravity field models and estimates of the geoid are useful for a wide range of research and application, including ocean circulation and climate change studies, physics of the earth's interior and height datum connection and unification. The computation of these models will require the solution of large and non-sparse normal equation systems, especially if "brute force" approaches are applied. Evidently there is a need for fast solvers. The multigrid approach is not only an extremely fast iterative solution technique, it yields en passant a well-defined sequence of coarser approximations as a by-product to the final gravity field solution. We investigate the implementation of multigrid methods to satellite data analysis using space-domain representations of the anomalous gravity field. Theoretical and numerical aspects are covered. Multigrid algorithms are applied as stand-alone solvers as well as for the construction of preconditioners in the conjugate gradient technique. Our numerical results, concerning a regional gravity inversion from simulated GRACE data, show that multigrid solvers run much faster than conjugate gradient solvers with conventional preconditioners.

Key words: Satellite gravity recovery – Multigrid method – Fast solvers – Regularization

1 Background

The Gravity Recovery and Climate Experiment (GRACE) and the Gravity Field and Steady-State Ocean Circulation Explorer (GOCE) satellite missions will provide gravity field information of unprecedented resolution and precision. It has been recognized that better gravity field models and estimates of the geoid are useful for a wide range of research and application, including ocean circulation and climate change studies, physics of the earth's interior and height datum connection and unification (ESA 1999; NRC 1997). The computation of these models from intersatellite–tracking and gradiometric data will require the solution of large normal equation systems[1]

$$\mathbf{N}\mathbf{x} = \mathbf{y} \tag{1}$$

where $\mathbf{x}$ is the vector of u unknown gravity field parameters, $\mathbf{N}$ the $u \times u$ normal matrix and $\mathbf{y}$ the right-hand side accumulated from satellite data. Numerical problems related to the computation of $\mathbf{N}$ and $\mathbf{y}$ itself will not be treated in this paper. Especially if "brute force" approaches are applied, $\mathbf{N}$ will be non-sparse. Moreover, due to the well-known ill-posed nature of the downward continuation process – the movement of satellites at orbital altitude smoothes out the fine structure of the gravity field – the normal matrices tend to be ill-conditioned. Also data gaps such as the polar regions in the GOCE mission are likely to deteriorate the condition numbers. Therefore we usually regularize the problem. Applying Tykhonov regularization with parameter α and matrix $\mathbf{M}$, the normals appear as

$$(\mathbf{N} + \alpha\mathbf{M})\mathbf{x} = \mathbf{y} \tag{2}$$

In GRACE and GOCE data analysis the size of the system of Eq. (1) or (2) will be of the order $u \approx 20.000 \ldots 90.000$, if we aim for global solutions. Besides, the optimal value of α is often not known a priori and has to be determined from parameter choice rules such as generalized cross-validation, the L-curve method or ridge regression techniques. Then Eq. (2) has to be solved several times and for condition numbers varying over several orders of magnitude. Fast iterative solvers must be designed to handle the problem within

[1] Within this paper, vectors and matrices are denoted by bold letters ($\mathbf{x}$), elements of function spaces by uppercase letters (X), and mappings on function spaces by calligraphic letters ($\mathcal{X}$)

acceptable computation time. A linear iteration of Eq. (1) or (2) reads (set $\mathbf{N} + \alpha\mathbf{M} =: \mathbf{N}^{\alpha}$)

$$\mathbf{x}^{k+1} = \mathbf{x}^{k} + \mathbf{C}(\mathbf{y} - \mathbf{N}^{\alpha}\mathbf{x}^{k}) \tag{3}$$

where $\mathbf{C}$ should approximate $(\mathbf{N}^{\alpha})^{-1}$, and it converges if and only if

$$\rho(\mathbf{I} - \mathbf{C}\mathbf{N}^{\alpha}) < 1 \tag{4}$$

The quantity ρ is the spectral radius of the iteration matrix, which is equal to the largest absolute value of the eigenvalues. A convergence rate $\rho = 0.1$, for example, means that one iteration step increases the accuracy of the solution by one numerical digit.

However, the actual convergence rate of iterative techniques strongly depends on the individual structure of the equation system under consideration, which, on the other hand, depends on the chosen gravity field representation, the numbering scheme for the unknowns, the satellite orbit altitude, the satellite data distribution, as well as the regularization parameter. Considering the case of space-domain gravity field representation, unfortunately the normal systems of Eqs. (1) or (2) lack a special block structure – which would make them suitable for block Jacobi techniques – as well as sparsity. In general, fast solvers for symmetric positive definite systems are Krylov methods such as the PCCGA (preconditioned conjugate gradient algorithm), and multigrid methods. The application of PCCGA and block-Jacobi techniques to gravity recovery from SST and SGG is discussed by Schuh et al. (1996) and Schuh (2000), where spherical harmonics are used as a basis. Moreaux (2000) uses truncated covariance functions in order to construct efficient preconditioners for Eq. (2) within the least-squares (LS) collocation approach. An iteration method for GOCE data analysis based on a problem-oriented approximative solver is presented in Klees et al. (2000). Kusche and Rudolph (2000) propose multigrid algorithms for gravity recovery using a space-domain representation.

In order to construct efficient multigrid solvers and preconditioners, it is necessary to go one step back and review the process of Galerkin discretization of the anomalous geopotential T. We assume that $T \in H$, where H is an infinite-dimensional Hilbert space equipped with a reproducing kernel $K = \sum_0^{\infty} \frac{2n+1}{4\pi} k_n P_n$. The reproducing kernel may be identified with a covariance function of T describing the state of knowledge of the geopotential power density. A linear operator $\mathscr{A}_{(n)} : H \to \mathbb{R}^n$ is supposed to map T onto n satellite observations l_i of SST or gradiometry type, $l_i + \epsilon_i = \mathscr{A}_i T = (A_i, T)_H$, $i = 1 \ldots n$. Here, $A_i \in H$ are the Riesz representers of the observation functionals. The regularized normal equations $(\mathscr{A}^*_{(n)}\mathscr{A}_{(n)} + \alpha\mathscr{I})T = \mathscr{A}^*_{(n)} l_{(n)}$ or

$$\mathscr{N}^{\alpha} T = Y \tag{5}$$

constitute a mapping of H onto itself, where $\mathscr{A}^*_{(n)}$ is the adjoint operator and $\mathscr{I}$ is the identity operator. For numerical purposes, Eq. (5) has to be discretized in the following. The most popular technique is Galerkin[2] LS projection. Looking for a solution T_j in a finite-dimensional subspace $H_j \in H$, we have to solve the H_j equations

$$\mathscr{N}^{\alpha}_j T_j = Y_j \tag{6}$$

where $\mathscr{N}^{\alpha}_j$ is the restriction of the normal equation operator and Y_j an orthogonal projection of the right-hand side (Kress 1989). Introducing a basis, $H_j = \mathrm{span}\{\Phi_i, i = 1 \ldots u_j\}$, and a weight matrix $\mathbf{P}$ for the observations, the normals finally take the well-known form of Eq. (2) with design matrix $\mathbf{A}_{ij} = \mathscr{A}_i\Phi_j = (A_i, \Phi_j)_H$, normal matrix $\mathbf{N} = \mathbf{A}^T\mathbf{P}\mathbf{A}$, right-hand side $\mathbf{y} = \mathbf{A}^T\mathbf{P}\mathbf{l}$, and Gramian regularization matrix $\mathbf{M}_{ij} = (\Phi_i, \Phi_j)_H$. Common choices for the basis of the approximation subspaces are the spherical harmonics $\Phi_j = Y_{jk}, k = -j \ldots j$, or a predefined system of harmonic kernel functions, $\Phi_j = \sum_0^{\infty} \frac{2n+1}{4\pi} \varphi_n P_n(\cdot, q_j)$, e.g. Stokes or Newton kernels. From the LS collocation point of view, the natural choice of the basis in H_j is given by the Riesz representers of the observation functionals, $\Phi_j = A_j, j = 1 \ldots n$. Here we end up with a Gramian matrix, $\mathbf{N}_{ij} = (A_i, A_j)_H$, and right-hand side data $\mathbf{y} = \mathbf{l}$. Concerning the huge amount of data collected during the GOCE and GRACE missions, we expect that only gridded or normal-point observations will be suitable to LS collocation processing. However, we assume that we need to regularize the LSC normal matrix.

Equations (6) are our point of departure in the derivation of multigrid iterative solvers. Multigrid algorithms have to be carefully adapted to the problem under consideration, but they often run much faster than Krylov methods with common algebraic preconditioners, or provide efficient preconditioners. Moreover, as a byproduct they yield a well-defined sequence of coarser approximations to the final solutions in hierarchically nested subspaces.

Although large-scale geodetic problems were already mentioned in a tutorial paper by Brandt (1982), one of the fathers of multigrid methods, these techniques apparently never gained attention in the geodetic literature. Therefore in Sect. 2 we recall the basic principles and few essential algorithms of multigrid methods. The remainder of this paper is organized as follows: Section 3 is devoted to the embedding of the multigrid concept in the framework of LS approximation on the sphere. Here we restrict ourselves to space-domain representations of the anomalous gravity field. In Sect. 4 we consider numerical questions related to the solution of satellite normals, using multi-grid methods as stand-alone iterative solvers. Their use as preconditioners in the conjugate gradient algorithm is described in Sect. 5. Finally, different algorithms are applied to a normal equation system resulting from a simulation of the GRACE mission scenario, and a summary of performance is given in Sect. 6. We conclude with an outlook. Convergence properties will be analysed in a follow-up paper.

[2]More precisely denoted as Galerkin–Bubnov discretization of the normal equations

2 The multigrid method

The multigrid approach was originally developed during the 1960s for the iterative solution of discrete elliptic boundary value problems. Multigrid iterations belong to the class of fastest iterations because their convergence rate is independent of the discretization, assuming that certain regularity assumptions are fulfilled. Introductory texts are those of Hackbusch (1985), Bramble (1993) or Braess (1996). Recent developments concern, for example, parallelization aspects of the multigrid approach. A couple of recent papers also deal with multilevel iterations for the solution of regularized ill-posed problems arising from first-kind integral equations, see Hanke and Vogel (1999) and the references therein. It was found that also in this case – which is indeed close to our application – multigrid techniques yielded very favourable convergence rates. In our presentation we follow Xu (1992), where the multigrid method is presented within a large group of multilevel techniques from a unified point of view.

The principle of multigrid iteration is simple: approximate solutions with smooth errors are obtained very efficiently by applying standard relaxation methods such as Richardson iteration, Jacobi overrelaxation (JOR), successive overrelaxation (SOR), symmetric SOR (SSOR), or block versions of these methods (Golub and van Loan 1983). Here smoothness means that the short wavelengths of the errors are reasonably damped, where the error is defined with respect to the exact discrete solution of the problem. Because of the error smoothness, corrections of these approximations can be calculated cheaply on coarser grids. By grids we mean hierarchically chosen approximation spaces $H_1 \subset \cdots \subset H_j \subset \cdots \subset H_J$. This basic idea can be used recursively employing coarser and coarser grids. Only on the coarsest grid must a direct solution be computed. The benefit of this principle, of course, also depends on the properties of the underlying equations and can hardly be forecasted for complex problems. The basic V-cycle algorithm for the H_j solution of the discretized equation

$$\mathscr{L}_j X_j = Y_j \tag{7}$$

with $\mathscr{L}_j : H_j \to H_j$, is as follows. The $(k+1)$-th iterate is given by

$$\begin{aligned} X_j^{k+1/3} &= X_j^k + \mathscr{S}_j\left(Y_j - \mathscr{L}_j X_j^k\right) \\ X_j^{k+2/3} &= X_j^{k+1/3} + \mathscr{R}_{j-1}\mathscr{Q}_{j-1}\left(Y_j - \mathscr{L}_j X_j^{k+1/3}\right) \\ X_j^{k+1} &= X_j^{k+2/3} + \mathscr{S}_j\left(Y_j - \mathscr{L}_j X_j^{k+2/3}\right) \\ &= X_j^k + \mathscr{R}_j\left(Y_j - \mathscr{L}_j X_j^k\right) \end{aligned} \tag{8}$$

By $\mathscr{Q}_{j-1}$ we denote the orthogonal projection onto H_{j-1}, and $\mathscr{S}_j$ is a suitable chosen relaxation operator with a smoothing property. Given X_j^k, the first step (presmoothing) provides a smoothed approximation in H_j. In the second step the remaining defect, which should be of long-wavelength nature, is restricted to H_{j-1}. We apply a coarse-grid correction using $\mathscr{R}_{j-1}$. Finally a post-smoothing is performed. It should be noted that the iteration operator $\mathscr{R}_j$ is defined recursively by $\mathscr{R}_{j-1}$. Only on the coarsest space the correction needs to be solved exactly: $\mathscr{R}_1 = (\mathscr{L}_1)^{-1}$. The algorithm of Eq. (8), applied with $j = J$ to the finest discretization in H_J, therefore makes use of all coarser approximation spaces down to H_1. The multigrid iteration process can be further accelerated by means of the concept of nested iteration: good initial approximations X_j^0 on each grid $H_j, i = 1 \ldots J$, can be found by performing a few multigrid steps, beginning with X_1^0. The initial coarse-space approximation "bootstraps" itself. Figure 1 indicates the principle for $J = 3$ grids, where the motivation for the name "V-cycle" becomes clear.

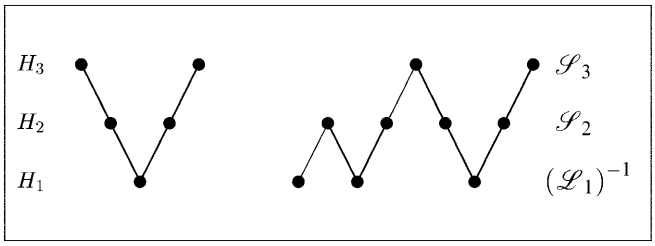

Fig. 1. Scheme of V-cycle, $J = 3$ (*left*), and nested iteration (*right*). $H_1 \subset H_2 \subset H_3$ are the approximation spaces. Each dot (•) indicates application of an operator: smoothing relaxation $\mathscr{S}_2$ and $\mathscr{S}_3$ on the fine- and intermediate grid, exact solution $(\mathscr{L}_1)^{-1}$ on the coarsest grid

The most crucial issue for the efficiency of multigrid algorithms is the approximation property: a Galerkin solution to Eq. (7) in H_{j-1} should be a good long-wavelength approximation to the Galerkin solution in H_j, therefore the coarser spaces have to be chosen in an appropriate way. This will be made more precise in Sect. 3. Convergence proofs are usually based on Sobolev norms adapted to the problem under consideration. In order to obtain an algebraic formulation, we introduce a basis $H_J = \operatorname{span}\{\Phi_{i(J)}, i = 1 \ldots u_J\}$, and Eq. (7) reads $\mathbf{L}_{(J)}\mathbf{x}_{(J)} = \mathbf{y}_{(J)}$, or simply[3] $\mathbf{L}\mathbf{x} = \mathbf{y}$. Within the algorithm of Eq. (8), a sequence of smaller auxiliary problems $\mathbf{L}_{(j)}\boldsymbol{\delta}\mathbf{x}_{(j)} = \mathbf{d}_{(j)}$ is solved instead. Due to $H_{j-1} \subset H_j$ it is clear that the base functions $\Phi_{i(j-1)}$ are spanned by the $\Phi_{i(j)}$

$$(\Phi_{1(j-1)}, \ldots, \Phi_{u_{j-1}(j-1)})^T = \mathbf{R}_{(j-1)}(\Phi_{1(j)}, \ldots, \Phi_{u_j(j)})^T \tag{9}$$

and the auxiliary systems are related by

$$\begin{aligned} \mathbf{L}_{(j-1)} &= \mathbf{R}_{(j-1)}\mathbf{L}_{(j)}\mathbf{R}_{(j-1)}^T \\ \mathbf{d}_{(j-1)} &= \mathbf{R}_{(j-1)}\mathbf{d}_{(j)} = \mathbf{R}_{(j-1)}(\mathbf{y}_{(j)} - \mathbf{L}_{(j)}\mathbf{x}_{(j)}) \end{aligned} \tag{10}$$

The corrections are canonically continued onto the finer space H_j

$$\boldsymbol{\delta}\mathbf{x}_{(j)} = \mathbf{R}_{(j-1)}^T\boldsymbol{\delta}\mathbf{x}_{(j-1)} \tag{11}$$

In other words, a linear interpolation is defined by Eq. (11). Obviously the $u_{j-1} \times u_j$ restriction matrices $\mathbf{R}_{(j-1)}$, $j = 2 \ldots J$, determine the efficiency of the algo-

[3] For vectors and matrices defined with respect to the finest discretization, we will frequently omit the level-indicating index (J)

rithm. They need to be sparse and are never stored as full matrices in order to avoid the matrix products in Eq. (10). Based on these considerations, a more flexible multigrid algorithm, which allows for different pre- and post-smoothing as well as multiple cycles between coarser levels, is as follows.

J-grid algorithm for the solution of $\mathbf{N}\mathbf{x} = \mathbf{y}$: (12)

Begin: Select $\mathscr{S}, \nu_1, \nu_2, \mathbf{x}^0$
Define $\mathbf{R}_{(j)}$
do $j = J-1, \ldots, 1$ $\mathbf{N}_{(j)} = \mathbf{R}_{(j)}\mathbf{N}_{(j+1)}\mathbf{R}_{(j)}^T$
do $k = 1, 2, \ldots$ $\mathbf{x}' = \mathscr{S}^{\nu_1}(\mathbf{x}^{k-1}, \mathbf{y}, \mathbf{N})$
$\mathbf{r}^{k-1} = \mathbf{N}\mathbf{x}' - \mathbf{y}$
$\mathbf{r}_{(J-1)} = \mathbf{R}_{(J-1)}\mathbf{r}^{k-1}$
$\boldsymbol{\delta}\mathbf{x}_{(J-1)}^0 = \mathbf{0}$
do $i = 1, 2, \ldots, \gamma$
if $J - 1 > 1$ then
$\boldsymbol{\delta}\mathbf{x}_{(J-1)}^i = \mathscr{M}(\boldsymbol{\delta}\mathbf{x}_{(J-1)}^{i-1}, \mathbf{r}_{(J-1)}, \mathbf{N}_{(J-1)})$
else if $J - 1 = 1$ then
Solve $\mathbf{N}_{(1)}\boldsymbol{\delta}\mathbf{x}_{(1)} = \mathbf{r}_{(1)}$
end if
end do
$\mathbf{x}'' = \mathbf{x}' - \mathbf{R}_{(J-1)}^T\boldsymbol{\delta}\mathbf{x}_{(J-1)}^{\gamma}$
$\mathbf{x}^k = \mathscr{S}^{\nu_2}(\mathbf{x}'', \mathbf{y}, \mathbf{N})$
$=: \mathscr{M}(\mathbf{x}^{k-1}, \mathbf{y}, \mathbf{N})$

By $\mathscr{S}^{\nu}$ we mean that a smoothing standard relaxation technique is applied ν times. Note that the new iterate $\mathscr{M}(\mathbf{x}^{k-1}, \mathbf{y}, \mathbf{N})$ on the J-level is defined in recursive style, since it involves the iterates $\mathscr{M}(\boldsymbol{\delta}\mathbf{x}_{(J-1)}^{i-1}, \mathbf{r}_{(J-1)}, \mathbf{N}_{(J-1)})$ of the defect corrections on the next-coarser level built in the same way. If we choose $\gamma > 1$, the algorithm of Eq. (12) cycles between coarser spaces. Figure 2 illustrates the basic cycles in the case of $J = 3$.

Considering the regularized normal equations Eq. (2), it seems quite obvious to apply the algorithm of Eq. (12) without modification to the regularized system.

J-grid algorithm for the solution of $(\mathbf{N} + \alpha\mathbf{M})\mathbf{x} = \mathbf{y}$: (13)

Begin: Set $\mathbf{N} := \mathbf{N} + \alpha\mathbf{M}$
and continue with the algorithm of Eq. (12)

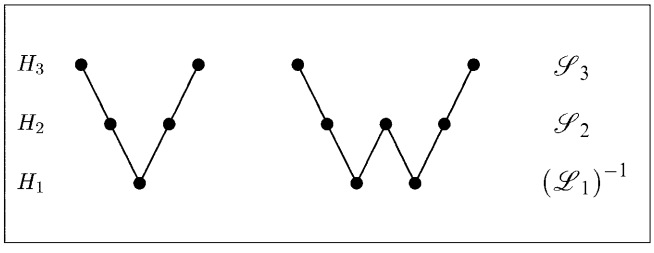

Fig. 2. Scheme of V-cycle, $J = 3$, $\gamma = 1$ (*left*); W-cycle, $\gamma = 2$ (*right*)

However, a regularized normal equation system may be always viewed as a discretization of a second-kind integral equation. This opens the door to the so-called multigrid methods of the second kind (Hackbusch 1985). The key issue is that an equation $(\mathbf{L} + \lambda\mathbf{I})\mathbf{x} = \mathbf{y}$ gives rise to the Picard-iteration $\mathbf{x}^{k+1} = \lambda^{-1}(\mathbf{y} - \mathbf{L}\mathbf{x}^k)$. Although such an iteration converges only if λ is even larger than the largest eigenvalue of $\mathbf{L}$ (and this means for unrealistic large values of the regularization parameter), it can be used as a smoothing technique. We obtain the following algorithm.

J-grid algorithm for the solution of $(\mathbf{N} + \alpha\mathbf{M})\mathbf{x} = \mathbf{y}$: (14)

Begin: Select $\mathbf{x}^0$
Define $\mathbf{R}_{(j)}$
do $j = J-1, \ldots, 1$ $\mathbf{N}_{(j)} = \mathbf{R}_{(j)}\mathbf{N}_{(j+1)}\mathbf{R}_{(j)}^T$
do $k = 1, 2, \ldots$ $\mathbf{r}^{k-1} = (\mathbf{N} + \alpha\mathbf{M})\mathbf{x}^{k-1} - \mathbf{y}$
Solve $\mathbf{M}\boldsymbol{\delta}\mathbf{x} = \alpha^{-1}\mathbf{r}^{k-1}$
$\mathbf{x}' = \mathbf{x}^{k-1} + \boldsymbol{\delta}\mathbf{x}$
$\mathbf{r}' = (\mathbf{N} + \alpha\mathbf{M})\mathbf{x}' - \mathbf{y}$
$\mathbf{r}_{(J-1)} = \mathbf{R}_{(J-1)}\mathbf{r}'$
$\boldsymbol{\delta}\mathbf{x}_{(J-1)}^0 = \mathbf{0}$
do $i = 1, 2, \ldots, \gamma$
if $J - 1 > 1$ then
$\boldsymbol{\delta}\mathbf{x}_{(J-1)}^i = \mathscr{M}(\boldsymbol{\delta}\mathbf{x}_{(J-1)}^{i-1}, \mathbf{r}_{(J-1)}, \mathbf{N}_{(J-1)})$
else if $J - 1 = 1$ then
Solve $(\mathbf{N}_{(1)} + \alpha\mathbf{M}_{(1)})\boldsymbol{\delta}\mathbf{x}_{(1)} = \mathbf{r}_{(1)}$
end if
end do
$\mathbf{x}^k = \mathbf{x}' - \mathbf{R}_{(J-1)}^T\boldsymbol{\delta}\mathbf{x}_{(J-1)}^{\gamma}$
$=: \mathscr{M}(\mathbf{x}^{k-1}, \mathbf{y}, \mathbf{N} + \alpha\mathbf{M})$

The regularization matrix $\mathbf{M}$ is usually band-limited or diagonally dominant, so that the solution of $\mathbf{M}\boldsymbol{\delta}\mathbf{x} = \alpha^{-1}\mathbf{r}^{k-1}$ should be determined without problems, or else be sufficiently well approximated. Finally, compared with the algorithm of Eq. (13), we see that Eq. (14) needs only one control parameter γ.

We conclude this chapter with a very simple and quite academic one-dimensional example in order to illustrate the procedures of Eqs. (13) and (14). The unknown function f in our example, which may be thought as an anomaly of a geophysical quantity defined along a profile, will be discretized by some locally supported base functions or finite elements $\phi_i, i = 1, \ldots, 4$.

Collecting a number of measurements, we set up the 4×4 normal system $(\mathbf{N} + \alpha\mathbf{M})\mathbf{x} = \mathbf{y}$ or $\mathbf{N}^\alpha\mathbf{x} = \mathbf{y}$. We assume that the problem is ill-posed due to the nature of the observations and needs to be regularized. Our aim is to solve the problem using two levels, $J = 2$. Accounting for geographical correlation, it makes sense to define the coarse-grid base functions simply by

$$\left(\phi_{1(1)}, \phi_{2(1)}\right)^T = \begin{pmatrix} \frac{1}{2} & \frac{1}{2} & 0 & 0 \\ 0 & 0 & \frac{1}{2} & \frac{1}{2} \end{pmatrix} \left(\phi_{1(2)}, \phi_{2(2)}, \phi_{3(2)}, \phi_{4(2)}\right)^T$$

The matrix above is the restriction matrix $\mathbf{R} = \mathbf{R}_{(1)}$. Note that this step requires at least a certain knowledge of the underlying problem. Assuming orthonormality of $\phi_i = \phi_{i(2)}$, we have the Gram matrix $\mathbf{M} = \mathbf{I}$, and the regularized 2×2 coarse-grid matrix is $\mathbf{N}_{(1)} + \alpha\mathbf{M}_{(1)} = \mathbf{R}\mathbf{N}\mathbf{R}^T + \frac{\alpha}{2}\mathbf{I}$. At this point we can already give the LS approximation of f in the coarser space $H_1 = \text{span}\{\phi_{i(1)}, i = 1, 2\}$

$$f_{(1)} = \left(\phi_{1(1)}, \phi_{2(1)}\right)\left(\mathbf{R}\mathbf{N}\mathbf{R}^T + \frac{\alpha}{2}\mathbf{I}\right)^{-1}\mathbf{R}\mathbf{y}$$

Next, in the course of the algorithm of Eq. (13) we have to choose a smoothing operator $\mathscr{S}$ which lives on the fine grid (or approximation space $H_2 = \text{span}\{\phi_{i(2)}, i = 1, \ldots, 4\}$). For the well-known Jacobi relaxation, for example, $\mathscr{S}(\mathbf{x}^{k-1}, \mathbf{y}, \mathbf{N}^\alpha) = \mathbf{x}^{k-1} + \mathbf{C}_{\text{Jac}}(\mathbf{y} - \mathbf{N}^\alpha\mathbf{x}^{k-1})$, with $\mathbf{C}_{\text{Jac}} = \text{diag}(1/\mathbf{N}^\alpha_{ii})$. In the algorithm of Eq. (14) the smoothing operation is performed implicitly by the Picard iteration matrix $\mathbf{C}_{\text{Pic}} = \alpha^{-1}\mathbf{I}$. The following coarse-grid correction step reads in both Eqs. (13) and (14) $\mathbf{x}^k = \mathbf{x}' + \mathbf{C}_{\text{cgc}}(\mathbf{y} - \mathbf{N}^\alpha\mathbf{x}')$ with $\mathbf{C}_{\text{cgc}} = \mathbf{R}^T(\mathbf{R}\mathbf{N}\mathbf{R}^T + \frac{\alpha}{2}\mathbf{I})^{-1}\mathbf{R}$. The new iterate $x^k = \mathscr{M}(\mathbf{x}^{k-1}, \mathbf{y}, \mathbf{N}^\alpha)$, combining smoothing and coarse-grid correction, is therefore given by

$$\begin{aligned}\mathscr{M}(\mathbf{x}^{k-1}, \mathbf{y}, \mathbf{N}^\alpha) = \mathscr{S}(\mathbf{x}^{k-1}, \mathbf{y}, \mathbf{N}^\alpha) \\ + \mathbf{C}_{\text{cgc}}(\mathbf{y} - \mathbf{N}^\alpha\mathscr{S}(\mathbf{x}^{k-1}, \mathbf{y}, \mathbf{N}^\alpha))\end{aligned}$$

Finally, in order to give a comparison in terms of convergence rates, we assume the normal matrix of our example to be of special Toeplitz structure with

$$\mathbf{N}_{ij} = 1 - \frac{|i-j|}{4} \quad i, j = 1 \ldots 4$$

Using regularization with $\alpha = \text{trace}(\mathbf{N})/\text{trace}(\mathbf{M}) = 1$, we have for pure Jacobi relaxation $\rho(\mathbf{I} - \mathbf{C}_{\text{Jac}}\mathbf{N}^\alpha) = 0.89$, whereas the two-level iterations of Eqs. (13) and (14) yield spectral radii of $\rho((\mathbf{I} - \mathbf{C}_{\text{cgc}}\mathbf{N}^\alpha)(\mathbf{I} - \mathbf{C}_{\text{Jac}}\mathbf{N}^\alpha)) = 0.39$ and $\rho((\mathbf{I} - \mathbf{C}_{\text{cgc}}\mathbf{N}^\alpha)(\mathbf{I} - \mathbf{C}_{\text{Pic}}\mathbf{N}^\alpha)) = 0.23$. Even without regularization, $\alpha = 0$, the algorithm of Eq. (13) still converges, whereas pure Jacobi relaxation diverges! The price to be paid is the additional complexity required by the formation and solution of the coarse-level system.

3 Spherical context

Here the basic concepts presented in the previous section will be embedded in the framework of LS approximation on the sphere. We assume that our fine-level approximation space H_J will be spanned by a basis of radial-symmetric harmonic functions $\Phi_{k(J)} \in H$ defined on a suitable chosen Bjerhammar sphere Ω, which allow the following Legendre series representation:

$$\Phi_{k(J)} = \Phi_{(J)}(\cdot, q_k) = \sum_{n=0}^{\infty} \frac{2n+1}{4\pi}\, \varphi_n^J\, P_n(\cdot, q_k) \quad k = 1 \ldots u_J \tag{15}$$

where P_n are the Legendre polynomials, φ_n^J the Legendre coefficients, and $q_k \in \Omega, k = 1 \ldots u_J$ is a set of points on the sphere. It seems natural to assume that the entries of the restriction matrices in Eq. (9) will be taken from some spherical radial-symmetric L^2 functions

$$\begin{aligned}\mathbf{R}_{ik(j-1)} = R_{(j-1)}(q_i, q_k) = \sum_{n=0}^{\infty} \frac{2n+1}{4\pi} r_n^{j-1} P_n(q_i, q_k) \\ i = 1 \ldots u_{j-1}, \;\; k = 1 \ldots u_j\end{aligned} \tag{16}$$

which should be of local support in order to minimize the computational burden. Nevertheless, the base functions $\Phi_{k(j)}, j < J$, defining the coarser approximation spaces are in general not radial-symmetric. Assuming u_J to be large for the moment, the restriction equation, Eq. (9), applied to the fine-level basis $\Phi_{k(J)}$ may be regarded as an approximate convolution integral

$$\begin{aligned}\Phi_{i(J-1)} &= \sum_{k=1}^{u_J} R_{(J-1)}(q_i, q_k)\Phi_{k(J)} \\ &= \int_{\Omega} R_{(J-1)}(q_i, q')\Phi_{(J)}(\cdot, q')\mathrm{d}\omega' + D \\ &= \sum_{n=0}^{\infty} \frac{2n+1}{4\pi}\, r_n^{J-1}\, \varphi_n^J P_n(\cdot, q_i) + D\end{aligned} \tag{17}$$

and similar relations hold for $\Phi_{k(j)}, j < J-1$. The magnitude of the error or discrepancy term D depends on the chosen point-set configuration, the number of points, as well as the smoothness of the functions $\Phi_{i(J)}$ and $R_{(J-1)}$. Error bounds are given in Freeden et al. (1998). Clearly, the base functions on the coarser levels of approximation tend towards low-pass filtered versions of the original H_J function, if the point-sets are sufficiently large.

Now let T_J be an approximation of the anomalous potential in H_J, and let $\mathscr{Q}_{J-1}T_J$ denote its H-orthogonal projection onto the coarser space $H_{J-1} = \text{span}(\Phi_{i(J-1)}, i = 1 \ldots u_{J-1})$, i.e.

$$(T_J, U_{J-1})_H = (\mathscr{Q}_{J-1}T_J, U_{J-1})_H \tag{18}$$

holds for arbitrary $U_{J-1} \in H_{J-1}$. Inserting Eq. (9) we obtain for an error bound

$$\begin{aligned}&||T_J - \mathscr{Q}_{J-1}T_J||_H \\ &\quad \le ||\mathbf{I} - \mathbf{R}^T_{(J-1)}(\mathbf{R}_{(J-1)}\mathbf{M}\mathbf{R}^T_{(J-1)})^{-1}\mathbf{R}_{(J-1)}\mathbf{M}|| \cdot ||T_J||_H\end{aligned} \tag{19}$$

where the matrix norm corresponds to $||\cdot||_H$ and

$$\mathbf{M}_{kl} = (\Phi_{k(J)}, \Phi_{l(J)})_H = \sum_{n=0}^{\infty} \frac{2n+1}{4\pi} \frac{(\varphi_n^J)^2}{k_n} P_n(q_k, q_l) \tag{20}$$

is of Gram type. It is obvious that for a given subspace dimension u_{J-1} the restriction matrix of Eq. (16) should be chosen such that a low error bound of Eq. (19) is obtained. As is well known, in the collocation case $\Phi_{i(J)} = K(q_i, \cdot)$, Eq. (20) reduces to $\mathbf{M}_{kl} = K(q_k, q_l)$. However, it seems difficult to improve the error estimate of Eq. (19) for general point-set configurations.

4 Solution of satellite normal equations by multigrid methods

Here we consider certain practical questions related to the construction of multigrid stand-alone solvers for Eq. (1) or (2). Our numerical example refers to regional recovery of gravity anomalies from intersatellite tracking data, so first we present the underlying recovery technique. Based on the Stokes–Pizzetti formula, we have a representation of the anomalous gravity field

$$T = \frac{R_e}{4\pi} \int_{\Omega} \delta g S(\cdot, q') \mathrm{d}\omega' \tag{21}$$

where R_e is the mean radius of the Earth, $S(\cdot, q')$ is the extended Stokes function, and δg are generally surface gravity anomalies (Heiskanen and Moritz 1967). In our case, they should be considered as residual, referring to a chosen reference field and defined on a reference surface (Bjerhammar sphere). If we discretize the anomaly function using u_J block-mean values, Eq. (21) can be approximated by

$$T_J = \frac{R_e}{4\pi} \sum_{i=1}^{u_J} \delta g_i S(\cdot, q_i) \Delta\Omega_i \tag{22}$$

where $\Delta\Omega_i = \int_{\Delta\omega_i} \mathrm{d}\omega'$. With $\Phi_i = R_e \Delta\Omega_i / (4\pi) S(\cdot, q_i)$ we have a representation of the type of Eq. (15), where the Legendre coefficients of the Stokes function equal $\varphi_n^J = R_e/(n-1)$. This has been used in a number of studies on regional gravity field recovery. If the anomaly blocks are chosen as equi-angular with respect to the geographical coordinate system, the midpoints q_i constitute a geographical grid of width Δ. For GRACE and GOCE data analysis, Δ between 0.5 and 2° seems appropriate. Coarser grids for our multigrid algorithms can be obtained easily by doubling the grid width: $2 \cdot \Delta$, $4 \cdot \Delta$, etc.

A popular numbering scheme for the unknown anomalies is latitude-by-latitude; see the left-hand side in Fig. 3. Numerical tests have shown, however, that this scheme is clearly not optimal if Gauss–Seidel-derived smoothers are applied within the multigrid algorithm (Rudolph 2000). The reason lies in the fact that these methods successively improve the unknowns, but the popular scheme causes jumps between algebraically neighbouring unknowns where the use of already improved unknowns looses its sense. Better-suited schemes are depicted in Fig. 3, in the centre and on the right-hand side. The scheme on the right-hand side is useful for domain partitioning and parallel computing.

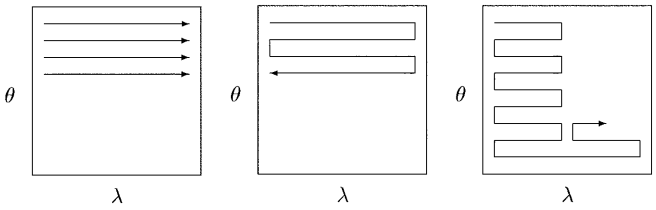

Fig. 3. Numbering schemes for anomaly blocks

Assuming that satellite measurements $l_i + \epsilon_i = \mathscr{A}_i T$, $i = 1 \ldots n$, are given, the normal matrix in Eqs. (1) and (2) is $\mathbf{N} = \mathbf{A}^T \mathbf{P} \mathbf{A}$, where the design $\mathbf{A}$ matrix usually contains certain derivatives of the Stokes function and $\mathbf{P}$ is a weight matrix which can be chosen from prior investigations on the measurement error's power spectral density. $\mathbf{x}$ is the vector of unknown mean gravity anomalies δg_i, and the right-hand side $\mathbf{y} = \mathbf{A}^T \mathbf{l}$ has to be accumulated from the data set. Numerous studies show that the normals need to be regularized – or prior information has to be added – from the LSC point of view. The choice of regularization parameter α and matrix $\mathbf{M}$ or measures to reduce discretization errors or the effect of omission zones will not be discussed in this paper; for more details see Xu (1992), Xu and Rummel (1994) and Ilk et al. (1995).

The multigrid algorithms of Eqs. (12), (13) or (14) may safely be stopped when the iteration error is significantly below the expected accuracy of the gravity field solution. An estimate for the iteration error is

$$||\mathbf{x}^k - \mathbf{x}|| \leq C = \frac{\rho}{1-\rho} ||\mathbf{x}^k - \mathbf{x}^{k-1}|| \tag{23}$$

where ρ is the convergence rate of the linear iteration process. Instead of computing ρ from the eigenvalues of the iteration matrix, it is common to estimate the quantity by the so-called reduction factor

$$\tilde{\rho} = ||\mathbf{x}^k - \mathbf{x}^{k-1}|| / ||\mathbf{x}^{k-1} - \mathbf{x}^{k-2}|| \tag{24}$$

An arbitrary norm can be chosen in Eqs. (23) and (24).

But even before the multigrid process terminates, it produces some interesting results. Within the nested iteration (cf. Fig. 1), exact solutions $\mathbf{x}_{(J-1)}, \mathbf{x}_{(J-2)}, \ldots$ on the coarser approximation spaces can be obtained. On the next-coarsest space with $2 \cdot \Delta$ resolution, for example, the solution vector $\mathbf{x}_{(J-1)} = (\delta g_{1(J-1)}, \ldots, \delta g_{u_{J-1}(J-1)})^T$ of the auxiliary system

$$\begin{aligned} &\mathbf{R}_{(J-1)} \mathbf{N}^{\alpha} \mathbf{R}_{(J-1)}^T \mathbf{x}_{(J-1)} \\ &\quad = (\mathbf{R}_{(J-1)} \mathbf{N} \mathbf{R}_{(J-1)}^T + \alpha \mathbf{R}_{(J-1)} \mathbf{M} \mathbf{R}_{(J-1)}^T) \mathbf{x}_{(J-1)} \\ &\quad = \mathbf{R}_{(J-1)} \mathbf{y} \end{aligned} \tag{25}$$

provides a regularized LS solution for the smoothed gravity field representation

$$T_{J-1} = \frac{R_e}{4\pi} \sum_{i=1}^{u_{J-1}} \delta g_{i(J-1)} \left(\sum_{k=1}^{u_J} R(q_i, q_k) S(\cdot, q_k) \Delta\Omega_k \right) \qquad (26)$$

In contrast, the restriction $\bar{\mathbf{x}}_{(J-1)} = \mathbf{R}_{(J-1)}\mathbf{x}$ of the final solution $\mathbf{x}$ computes weighted regional means over the gravity anomaly function

$$\overline{T}_{J-1} = \frac{R_e}{4\pi} \sum_{i=1}^{u_{J-1}} \left(\sum_{k=1}^{u_J} R(q_i, q_k)\ \delta g_k \right) S(\cdot, q_i)\ \Delta\Omega_i \qquad (27)$$

Within this study, we use a computationally simple normalized three-step restriction function

$$R_{(j-1)}(q_i, q_k) = \begin{cases} a & \text{if } \psi_{ik} = 0 \\ b & \text{if } 0 < \psi_{ik} \le \Delta_j \\ c & \text{if } \Delta_j < \psi_{ik} \le \sqrt{2}\Delta_j \\ 0 & \text{if } \sqrt{2}\Delta_j < \psi_{ik} \end{cases} \quad \sum_{k=1}^{u_j} R(\cdot, q_k) = 1 \qquad (28)$$

where $\psi_{ik} = \sphericalangle(q_i, q_k)$ denotes the spherical distance between points q_i and q_k, Δ_j the grid width in H_j, and $a \ge b \ge c > 0$. As mentioned before, we do not store the restriction coefficients $\mathbf{R}_{(j-1)}$ as full matrices. Instead, using the compressed matrix storage mode (Björck 1996), only the few non-zero entries are held in the computer memory – less than 0.2% in our numerical example due to the short cut-off distance $\sqrt{2}\Delta_j$, in Eq. (28). The principle is depicted in Fig. 4, where s is the maximum possible number of non-zero entries per each q_i due to Eq. (28). In the numerical example of Sect. 6 we have $s = 9$.

5 Multigrid preconditioner

Efficient Krylov solvers such as the conjugate gradient method require a preconditioning strategy, if applied to an equation system of bad condition such as Eqs. (1) or (2). By preconditioning we mean (Golub and van Loan 1983; Hackbusch 1993) that each CG step begins with the solution of a linear equation system

$$\mathbf{C}\boldsymbol{\rho}^{k-1} = \mathbf{r}^{k-1} \qquad (29)$$

where $\mathbf{r}^{k-1} = (\mathbf{N} + \alpha\mathbf{M})\mathbf{x}^{k-1} - \mathbf{y} = \mathbf{N}^{\alpha}\mathbf{x}^{k-1} - \mathbf{y}$ is the residual vector and $\mathbf{C}$ the symmetric and positive definite preconditioner. In the case of PCCGA, each iteration step damps the error by $2(\sqrt{\kappa(\mathbf{C}^{-1}\mathbf{N}^{\alpha})} - 1)/(\sqrt{\kappa(\mathbf{C}^{-1}\mathbf{N}^{\alpha})} + 1)$, therefore a good preconditioner should reduce the condition number κ but, on the other hand, should allow fast solution of Eq. (29). A popular choice is the diagonal preconditioner, $\mathbf{C} = \mathrm{diag}(\mathbf{N}^{\alpha}_{ii})$. If we apply m cycles of a symmetric multigrid iteration to the system

$$\mathbf{N}^{\alpha}\boldsymbol{\rho} = \mathbf{r}^{k-1} \qquad (30)$$

beginning with $\boldsymbol{\rho}^0 = \mathbf{0}$, the preconditioner $\mathbf{C}$ is given implicitly by the mth power of the multigrid iteration matrix, and the preconditioned residual $\boldsymbol{\rho}^{k-1}$ is the mth multigrid iterate $\boldsymbol{\rho}^m$ for the exact solution $\boldsymbol{\rho}$ of Eq. (30). Multigrid preconditioning, however, can be viewed from a different point of view: as a multigrid iteration process, each m steps combined with a PCCGA step. We find that with multigrid-preconditioned CGA the stopping rule of Eqs. (23) and (24) works much less reliably than with multigrid stand-alone iterations, probably since PCCGA is basically not a linear iteration. The convergence rate itself, however, is clearly accelerated. More sophisticated error estimates can be found in, for example, Hackbusch (1993).

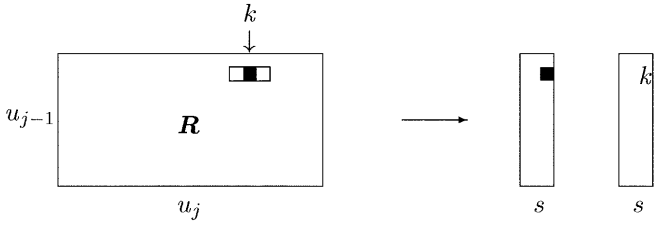

Fig. 4. Storing the restriction coefficients within the compressed matrix scheme. Only one $u_{j-1} \times s$ real array and one $u_{j-1} \times s$ integer array are needed. s is the maximum number of nonzero entries

6 A numerical example

A numerical example should demonstrate the application of multigrid stand-alone solution and preconditioning techniques to satellite gravity anomaly recovery. Satellite data $\mathbf{y}$ and normal matrix $\mathbf{N}$ were created within a simulation experiment following the GRACE mission scenario: a low–low high-precision intersatellite mission, based on the EGM96 spherical harmonic geopotential model for orbit (at 400 km altitude) and data simulation. An analysis period of 31 days was chosen. Intersatellite range-rate measurements were generated at a sampling rate of 0.2 Hz and corrupted with Gaussian white noise of variance $(1\ \mu\ \mathrm{m/s})^2$. This means that a total number of 53 500 simulated observations had to be processed. The methodology is presented in Ilk et al. (1995). The area under consideration was chosen to be $[57 \ldots 132°] \times [-24 \ldots 43°]$; see Fig. 5. A set of 5025 $1 \times 1°$ mean anomaly blocks, computed from the EGM96 model complete up to degree and order 360 and reduced by a low-degree reference model (OSU91 complete up to degree and order 12), is shown in Fig. 6. This does not mean that we expect to recover the gravity field at $1 \times 1°$ resolution with an S/N ratio of 1, but a high resolution was chosen in order to demonstrate algorithmic performance in a seriously ill-posed problem. The same example has been used in Kusche and Rudolph (2000). In order to simulate different degrees of ill-posedness – or accuracy of prior information from the LSC point of view – here the regularization parameter has been shifted additionally by some orders of magnitude.

In this example various algorithms were applied:

(1) MGV2JOR multigrid algorithm of Eq. (13), $J = 2$, with Jacobi overrelaxation (JOR) smoother

(2) MGV2R multigrid algorithm, Eq. (14), $J = 2$
(3) MGV3JOR multigrid algorithm, Eq. (13), $J = 3$, with JOR smoother, V-cycle, $\gamma = 1$
(4) MGW3JOR multigrid algorithm, Eq. (13), $J = 3$, with JOR smoother, W-cycle, $\gamma = 2$
(5) CGA-J conjugate gradient algorithm with diagonal preconditioner
(6) CGA-MGV2JOR conjugate gradient algorithm with $m = 2$ cycles of multigrid algorithm MGV2JOR as preconditioner
(7) CGA-MGV3JOR conjugate gradient algorithm with $m = 2$ cycles of multigrid algorithm MGV3JOR as preconditioner.

The coarser grids were obtained by standard coarsening, i.e. as $2 \times 2^\circ$ and $4 \times 4^\circ$ grids.

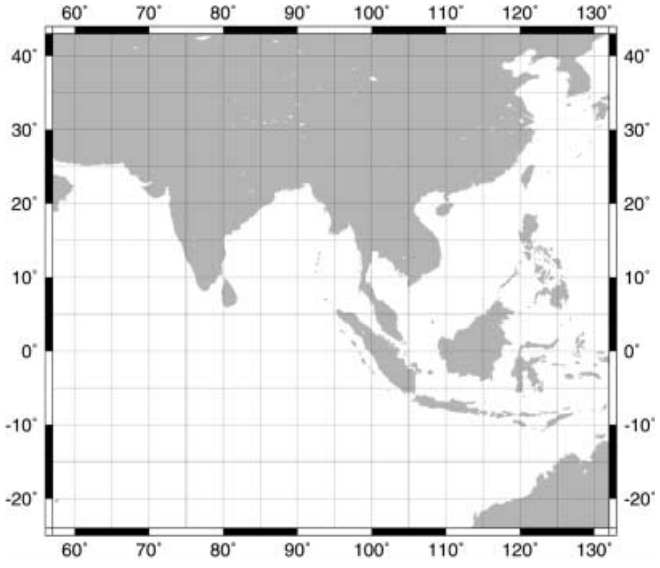

Fig. 5. Area under consideration

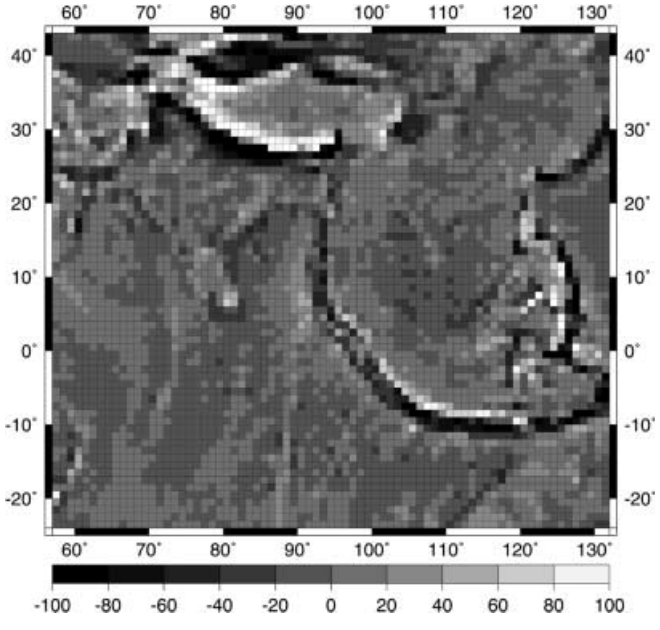

Fig. 6. (Pseudo-) true gravity anomalies (mGal)

The initial $4 \times 4^\circ$ approximation as well as the final $2 \times 2^\circ$ approximation obtained by nested iteration are shown in Figs. 7 and 8. The final $1 \times 1^\circ$ approximation from algorithm CGA-MGV2JOR after seven cycles is given in Fig. 9, where the estimated as well as the true iteration error is far below 0.1 mGal. When compared to the pseudo-true field (Fig. 6), we can observe that the main features are well detected. As expected, we cannot hope to recover the gravity field at such high resolution from a GRACE-type mission with satisfying S/N ratio. In particular, ocean-ridge features of alternating sign remain invisible within this experiment. We found a root mean square (RMS) error of 12 mGal in the $2 \times 2^\circ$

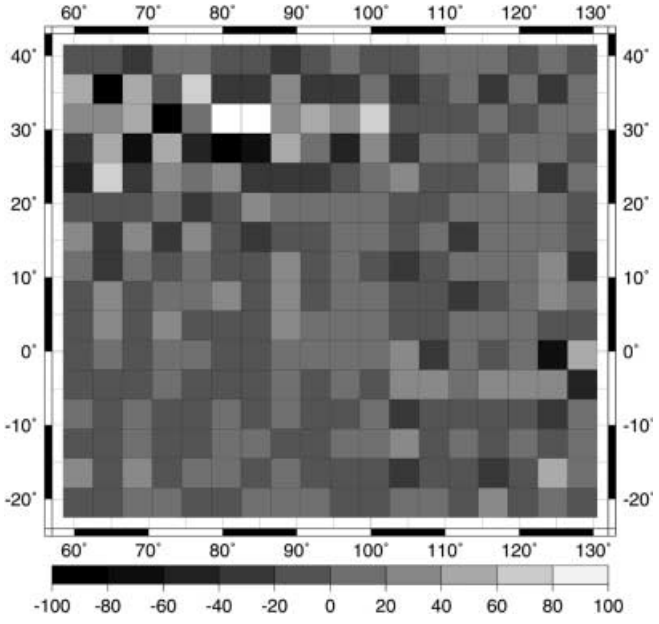

Fig. 7. Initial approximation on $4 \times 4^\circ$

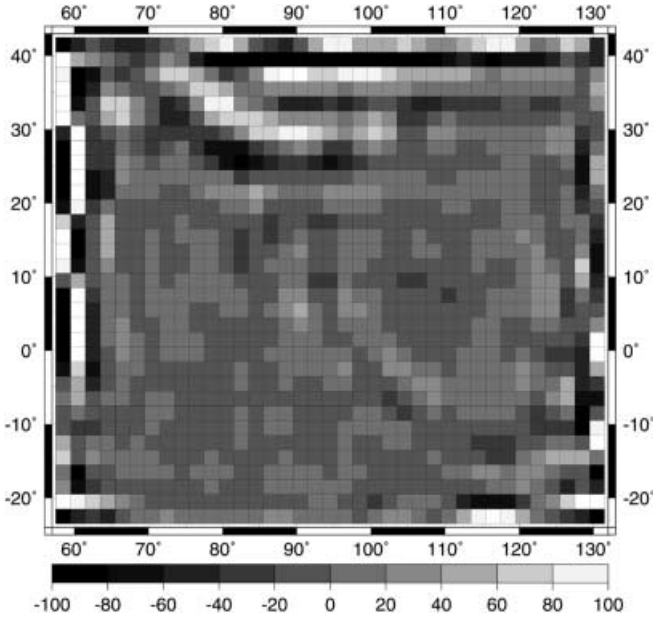

Fig. 8. Final approximation on $2 \times 2^\circ$

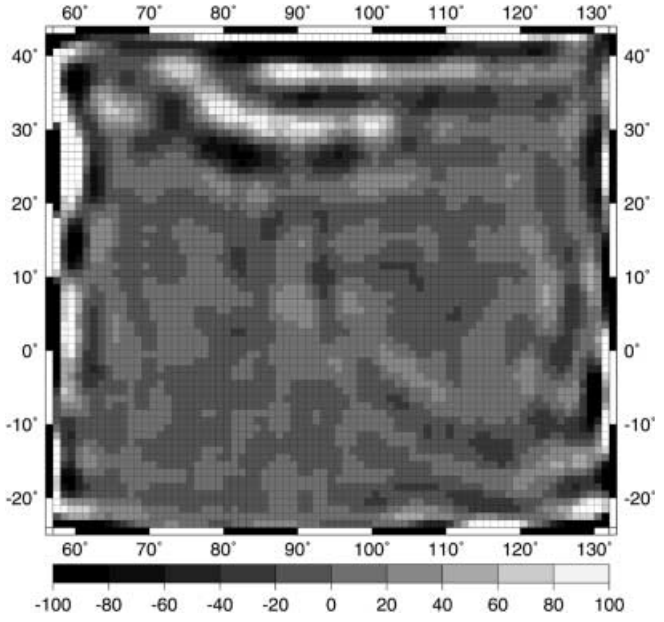

Fig. 9. Final approximation

block means weighted according to Eq. (27), and of 5 mGal in the weighted $4 \times 4^\circ$ block means, when comparing to the E6M96-derived weighted blocks. Here the regularization parameter was $\alpha = 1 \cdot 10^{10}$, which is small when compared to an average diagonal element trace $(\mathbf{N})/u = 3 \cdot 10^{11}$. However, the important result is that a suitable approximation is available after very few iteration cycles, which means far less than 1% of the computation time when compared to a direct solver.

A comparison of the different algorithms is given in Tables 1, 2 and 3.

α is the regularization parameter, Iter no. is the number of multigrid-cycles or CG-steps required by the algorithm, and Time the execution time on a SUN Ultra 1 in minutes. Each algorithm was terminated when the true RMS iteration error $||\mathbf{x} - \mathbf{x}^k||_2$ fell below 0.1 mGal. "Exact" solutions $\mathbf{x}$ of the regularized normal equations, which only serve as a reference within this study, have been derived for different αs from running CGA–MGV2JOR to $||\mathbf{r}||_2 < 1 \cdot 10^{-3}$. In the case of multigrid methods, C denotes the algorithm's self-estimate [Eq. (23)] for the RMS iteration error bound in mGal, which is usually very good.

If only two grids are implemented – which is generally favourable as long as a direct solution on the coarser space can be cheaply calculated – algorithms MGV2JOR and MGV2R run very fast as long as the problem is not too ill-conditioned. In the case of small regularization parameters, MGV2R based on Eq. (14) diverges due to large smoothing corrections. The use of three grids serves as a test case for large-scale application. Generally we found that the algorithms MGV3JOR and MGW3JOR were very sensitive to the specific configuration of the smoother, i.e. ν_1, ν_2 and overrelaxation parameter. We believe the reason for this is that also the auxiliary systems of Eq. (25) are of bad condition and require careful handling. Increasing the number of inner cycles γ did not further enhance the performance – due to the bad condition of the auxiliary systems we would usually need $\gamma > 10$ for a sufficiently accurate solution of the defect equation on the second grid, which makes the algorithm perform numerically like MGV2JOR but more time-consuming. However, we expect that MGV3JOR and MGW3JOR have great potential for large-scale application since only systems of a size less than $u/16$ need to be solved directly. The clear winner of this comparison is the conjugate gradient algorithm with multigrid preconditioning. We found that CGA-MGV2JOR was able to solve the normal equations within an acceptable time even for unrealistic strong ill-posedness, i.e. for very small regularization parameters. The conjugate gradient technique with conventional preconditioning such as diagonal (CGA-J) or (not shown in Table 3) SSOR can compete neither with multigrid stand-alone solvers (Table 1) nor with multigrid-preconditioned CG.

Table 1. Performance of different multigrid algorithms ($J = 2$). α is the regularization parameter, Iter no. the number of iteration steps, and Time the execution time on Ultra 1 in minutes. $\tilde{\rho}$ is the estimated convergence rate according to Eq. (24), and C the iteration error bound [Eq. (23)] in mGal estimated using $\tilde{\rho}$

α	MGV2JOR				MGV2R			
	Iter no.	Time	C	$\tilde{\rho}$	Iter no.	Time	C	$\tilde{\rho}$
1×10^{11}	5	6	0.08	0.38	5	6	0.05	0.23
5×10^{10}	11	10	0.09	0.66	6	7	0.12	0.32
1×10^{10}	61	41	0.09	0.91	37	25	1.23(!)	0.85
5×10^{9}	127	75	0.09	0.96	no convergence			

Table 2. Performance of different multigrid algorithms ($J = 3$)

α	MGV3JOR				MGW3JOR			
	Iter no.	Time	C	$\tilde{\rho}$	Iter no.	Time	C	$\tilde{\rho}$
1×10^{11}	9	12	0.18	0.54	8	12	0.05	0.52
5×10^{10}	14	16	0.10	0.72	14	17	0.09	0.72
1×10^{10}	79	71	0.09	0.93	79	79	0.09	0.93
5×10^{9}	165	140	0.10	0.96	164	155	0.10	0.96

Table 3. Performance of different conjugate gradient preconditioners

α	CGA-J		CGA-MGV2JOR		CGA-MGV3JOR	
	Iter no.	Time	Iter no.	Time	Iter no.	Time
1×10^{11}	55	23	3	7	5	14
5×10^{10}	78	33	4	9	5	14
1×10^{10}	180	71	7	13	12	26
5×10^{9}	260	104	10	16	17	37

7 Outlook

We found that multigrid methods offer a flexible and fast tool to compute gravity anomaly solutions from

regularized satellite normal equations, which will arise from the dedicated gravity missions of the present decade. We expect that global high-resolution solutions, based on space-domain gravity field representations, will be possible within acceptable computation time. Further investigations will concern convergence properties of multigrid algorithms as well as global application and parallelization aspects.

Acknowledgements. The author thanks Prof. H.-P. Helfrich for valuable discussions. Also the help of Prof. W. Keller and two anonymous reviewers is greatly appreciated.

References

Björck Å (1996) Numerical methods for least squares problems. SIAM, Philadelphia

Braess D (1996) Finite Elemente. Springer, Berlin Heidelberg New York

Bramble JH (1993) Multigrid methods. Pitman research notes in mathematics series, Harlow

Brandt A (1982) Guide to multigrid development. In: Hackbusch W, Trottenberg U (eds) Multigrid methods. Springer, Berlin Heidelberg New York

ESA (1999) Gravity field and steady-state ocean circulation mission. European space agency publications division, Reports for mission selection, ESA SP-1233(1), Noordwijk

Freeden W, Gervens T, Schreiner M (1998) Constructive approximation on the sphere. Clarendon, Oxford

Golub GH, van Loan C (1983) Matrix computations. John Hopkins University Press, Baltimore

Hackbusch W (1985) Multi-Grid methods and applications. Springer series in computational mathematics, Berlin

Hackbusch W (1993) Iterative solution of large sparse systems of equations. Springer applied mathematical Sciences, Berlin

Hanke M, Vogel CR (1999) Two-Level preconditioners for regularized inverse problems I: Theory. Num Math 83: 385–402

Heiskanen WA, Moritz H (1967) Physical geodesy. Freeman, San Francisco

Ilk KH, Rummel R, Thalhammer M (1995) Refined method for the regional recovery from GPS/SST and SGG. In: Study of the gravity field determination using gradiometry and GPS (phase 2). CIGAR III/2 final report, ESA Contract no. 10713/93/F/FL

Klees R, Koop R, Visser P, van den IJssel J, Rummel R (2000) Data analysis for the GOCE mission. In: Schwarz K-P (ed) Geodesy beyond year 2000. Proc IAG Gen Ass Birmingham. Springer, Berlin Heidelberg New York

Kress R (1989) Linear integral equations. Applied mathematical sciences. Springer, Berlin Heidelberg New York

Kusche J, Rudolph S (2000) The multigrid method for satellite gravity field recovery. In: Schwarz K-P (ed) Geodesy beyond year 2000. Proc IAG Gen Ass Birmingham. Springer, Berlin Heidelberg New York

Moreaux G (2000) Harmonic spherical splines with locally supported kernels. In: Schwarz K-P (ed) Geodesy beyond year 2000. Proc IAG Gen Ass Birmingham. Springer, Berlin Heidelberg New York

NRC (1997) Satellite gravity and the geosphere. National Academy Press, Washington, DC

Rudolph S (2000) Regionale und globale Gravitationsfeldanalyse hochauflösender Satellitendaten mittels Mehrgitterverfahren. Deutsche Geodätische Kommission, Reihe C, Nr. 528

Schuh W-D (2000) Scientific data processing algorithms. In: Sünkel H (ed) From eötvös to milligal. final report, ESA study, ESA/ESTEC Contract no. 13392/98/NL/GD

Schuh W-D, Sünkel H, Hausleitner W, Höck E (1996) Refinement of iterative procedures for the reduction of spaceborne gravimetry data. In: Study of advanced reduction methods for spaceborn gravimetry data, and of data combination with geophysical parameters. CIGAR IV final report, ESA study ESTEC/JP/95-4-137/MS/nr

Xu J (1992) Iterative methods by space decomposition and subspace correction. SIAM Rev 34(4): 581–613

Xu P (1992) Determination of surface gravity anomalies using gradiometric observables. Geophys J Int 110: 321–332

Xu P, Rummel R (1994) A Simulation study of smoothness methods in recovery of regional gravity fields. Geophys J Int 117: 472–486